

# Low-temperature studies of the magnetic and superconducting properties of the $R_2\text{Ir}_3\text{Si}_5$ ( $R=\text{Y, La, Ce-Nd, Gd-Tm}$ ) system

Yogesh Singh, D. Pal, and S. Ramakrishnan

*Tata Institute of Fundamental Research, Bombay-400005, India*

(Received 15 March 2004; revised manuscript received 5 April 2004; published 5 August 2004)

Polycrystalline samples of the ternary rare-earth silicide compounds  $R_2\text{Ir}_3\text{Si}_5$  ( $R=\text{Y, La, Ce-Nd, Gd-Tm}$ ) have been prepared and characterized using room temperature powder x-ray, magnetic susceptibility, electrical resistivity, and low-temperature (1.6–30 K) zero-field heat capacity measurements. All the compounds crystallize in the tetragonal  $\text{U}_2\text{Co}_3\text{Si}_5$  type structure (space group *Ibam*). The effective moments estimated from Curie-Weiss fits to the high-temperature inverse susceptibility data suggest that Ir may carry an induced moment in these compounds. The systematics of the lattice parameters across the series suggest that Ce is trivalent in  $\text{Ce}_2\text{Ir}_3\text{Si}_5$ , whereas the magnetic, transport, and heat capacity measurements reveal a nonmagnetic behavior for this compound, suggesting that this is a strongly hybridized compound similar to  $\text{Ce}_2\text{Rh}_3\text{Si}_5$ .  $\text{Pr}_2\text{Ir}_3\text{Si}_5$  also does not order down to 1.8 K. Large and prominent peaks at low temperatures in the susceptibility and heat capacity of the other magnetic rare-earth-containing compounds indicate bulk magnetic ordering of trivalent rare-earth moments in these compounds. The heat capacity data for  $\text{Gd}_2\text{Ir}_3\text{Si}_5$  show three anomalies, one above and one below the main  $\lambda$  type antiferromagnetic transition peak at 11.8 K, while the data for  $\text{Tb}_2\text{Ir}_3\text{Si}_5$  also suggest two transitions. Most of the compounds have transition temperatures which follow the de Gennes scaling. However,  $\text{Nd}_2\text{Ir}_3\text{Si}_5$  and  $\text{Tb}_2\text{Ir}_3\text{Si}_5$  have anomalously large transition temperatures compared to that expected by the de Gennes scaling. Large crystalline electric field effects are indicated by the reduced value of the magnetic entropy at 30 K, and this could be a possible reason for the deviation of the ordering temperature  $T_N$  from the de Gennes factor. From the temperature dependence of the magnetic entropy we conclude that  $\text{Nd}_2\text{Ir}_3\text{Si}_5$ ,  $\text{Tb}_2\text{Ir}_3\text{Si}_5$ ,  $\text{Dy}_2\text{Ir}_3\text{Si}_5$ , and  $\text{Ho}_2\text{Ir}_3\text{Si}_5$  are in a doublet ground state. The anomalies in the susceptibility and heat capacity near 2 K for  $\text{La}_2\text{Ir}_3\text{Si}_5$  and 2.9 K for  $\text{Y}_2\text{Ir}_3\text{Si}_5$  suggest that these compounds undergo a transition into the superconducting state at low temperatures. A reduced jump  $\Delta C/\gamma T_C$  at  $T_C$  and a large linear term in the temperature dependence of the heat capacity in the superconducting state are observed, and we compare this with similar behavior seen in the nonmagnetic superconducting members of the structurally related series  $R_2\text{Fe}_3\text{Si}_5$ , where it has been suggested that a fraction of the Fermi surface remains normal below  $T_C$ .

DOI: 10.1103/PhysRevB.70.064403

PACS number(s): 75.20.En, 75.40.Cx, 75.30.Kz, 74.70.Ad

## I. INTRODUCTION

Rare-earth ternary silicides and germanides of the  $R_2\text{T}_3\text{X}_5$  type, which form in a variety of crystal structures, have led to a number of studies due to their remarkable low-temperature physical properties.<sup>1–3</sup> The  $R_2\text{Fe}_3\text{Si}_5$  compounds, more than others, have been given a lot of attention due to their unusual magnetic and superconducting properties: the Lu compound superconducts below 6.2 K, a record high for an iron-containing compound, and the Tm compound is the only reentrant superconductor where superconductivity (at about 1.6 K) is destroyed by purely antiferromagnetic order at 1 K.<sup>3–6</sup> Another magnetic member of this series,  $\text{Er}_2\text{Fe}_3\text{Si}_5$ , has been recently reported to show superconductivity, where a zero in resistivity is attained at 0.47 K below incommensurate and commensurate antiferromagnetic transitions at 2.8 K and 2.4 K, respectively.<sup>7</sup> Compared to the  $R_2\text{Fe}_3\text{Si}_5$  series, compounds of the type  $R_2(\text{Ir, Rh, Ni})_3(\text{Si, Ge, Sn})_5$ , which form in structures related to the  $R_2\text{Fe}_3\text{Si}_5$  structure, have not been studied in any detail. We have in the recent past been investigating in detail the magnetic, transport, and thermodynamic properties of these compounds.<sup>8–12</sup> The coexistence of superconductivity and antiferromagnetism in  $\text{Tm}_2\text{Rh}_3\text{Sn}_5$ ,<sup>10</sup> the possible super-

conductivity in  $\text{Tm}_2\text{Rh}_3\text{Si}_5$ ,<sup>9</sup> the presence of both trivalent and divalent Yb in the Kondo lattice compound  $\text{Yb}_2\text{Ir}_3\text{Ge}_5$ ,<sup>11</sup> the change of structure and semiconducting resistivity behavior in the series of compounds  $R_2\text{Ir}_3\text{Ge}_5$  for  $R$  heavier than Dy (Ref. 12) are just some of the interesting results which have come out of these investigations. As part of our continuing effort to investigate the 235 system, here we report our detailed magnetic susceptibility, electrical resistivity, and low-temperature heat capacity results for polycrystalline samples of the series of compounds  $R_2\text{Ir}_3\text{Si}_5$  ( $R=\text{Y, La, Ce-Nd, and Gd-Tm}$ ). To the best of our knowledge, only  $\text{Y}_2\text{Ir}_3\text{Si}_5$  (Ref. 13) and  $\text{Ce}_2\text{Ir}_3\text{Si}_5$  (Ref. 14) have been reported on earlier.

## II. EXPERIMENTAL DETAILS

Polycrystalline samples of  $R_2\text{Ir}_3\text{Si}_5$  ( $R=\text{Y, La, Ce-Nd, and Gd-Tm}$ ) were prepared by the usual arc melting on a water-cooled copper hearth in an atmosphere of continuously flowing argon. The purity of the rare-earth metals and Ir was 99.9% whereas the purity of Si was 99.999%. The resulting ingots were flipped over and remelted five to six times to ensure homogeneous mixing. The samples were

TABLE I. Lattice parameters of  $R_2\text{Ir}_3\text{Si}_5$ .

Sample	$a$ (Å)	$b$ (Å)	$c$ (Å)
$\text{Y}_2\text{Ir}_3\text{Si}_5$	$9.918 \pm 0.005$	$11.472 \pm 0.005$	$5.795 \pm 0.005$
$\text{La}_2\text{Ir}_3\text{Si}_5$	$9.979 \pm 0.005$	$11.649 \pm 0.005$	$5.924 \pm 0.005$
$\text{Ce}_2\text{Ir}_3\text{Si}_5$	$9.960 \pm 0.005$	$11.629 \pm 0.005$	$5.879 \pm 0.005$
$\text{Pr}_2\text{Ir}_3\text{Si}_5$	$9.947 \pm 0.005$	$11.615 \pm 0.005$	$5.872 \pm 0.005$
$\text{Nd}_2\text{Ir}_3\text{Si}_5$	$9.939 \pm 0.005$	$11.587 \pm 0.005$	$5.857 \pm 0.005$
$\text{Gd}_2\text{Ir}_3\text{Si}_5$	$9.925 \pm 0.005$	$11.521 \pm 0.005$	$5.822 \pm 0.005$
$\text{Tb}_2\text{Ir}_3\text{Si}_5$	$9.916 \pm 0.005$	$11.487 \pm 0.005$	$5.799 \pm 0.005$
$\text{Dy}_2\text{Ir}_3\text{Si}_5$	$9.897 \pm 0.005$	$11.406 \pm 0.005$	$5.779 \pm 0.005$
$\text{Ho}_2\text{Ir}_3\text{Si}_5$	$9.883 \pm 0.005$	$11.371 \pm 0.005$	$5.759 \pm 0.005$
$\text{Er}_2\text{Ir}_3\text{Si}_5$	$9.872 \pm 0.005$	$11.364 \pm 0.005$	$5.751 \pm 0.005$
$\text{Tm}_2\text{Ir}_3\text{Si}_5$	$9.866 \pm 0.005$	$11.330 \pm 0.005$	$5.745 \pm 0.005$

wrapped in Zr foils and vacuum annealed at 900 °C for a period of 10 days. The room temperature x-ray powder diffraction pattern of all the samples could be indexed to the tetragonal  $\text{U}_2\text{Co}_3\text{Si}_5$  type structure. The lattice constants have been listed in Table I. The lattice parameters are seen to decrease more or less linearly with increasing occupation  $n$  of the  $4f$  shell of the trivalent rare-earth ions. This is the expected lanthanide contraction commonly observed in  $R$ -based compounds. It can be seen that the lattice constants for the Ce compound do not exhibit any obvious anomaly, which suggests that Ce atoms in this system may be trivalent or nearly trivalent at least at 300 K. To the best of our knowledge only the compounds  $\text{Y}_2\text{Ir}_3\text{Si}_5$  (Ref. 13) and  $\text{Ce}_2\text{Ir}_3\text{Si}_5$  (Ref. 14) of this series have been reported on, and our estimated lattice parameters for these compounds compare well with the earlier reported values. The dc magnetic susceptibility ( $\chi$ ) as a function of the temperature was measured using a commercial superconducting quantum interference device magnetometer in a field of 10 Oe (for superconducting samples) and 1 kOe (for magnetic samples) in the temperature range from 1.8 to 300 K. The resistance was measured in the temperature range 1.5 K to 300 K by the usual four-contact method using an LR-700 resistance bridge. The heat capacity in zero field between 1.7 K and 30 K was measured with an accuracy of 1% using an automated adiabatic heat pulse calorimeter. A calibrated germanium resistance thermometer (Lake Shore Inc., USA) was used as the temperature sensor in this range.

### III. RESULTS AND DISCUSSION

#### A. Magnetic susceptibility studies

##### 1. Properties of $\text{La}_2\text{Ir}_3\text{Si}_5$ and $\text{Y}_2\text{Ir}_3\text{Si}_5$

The temperature dependence of the dc magnetic susceptibility ( $\chi$ ) of  $\text{Y}_2\text{Ir}_3\text{Si}_5$  and  $\text{La}_2\text{Ir}_3\text{Si}_5$  at low temperatures is shown in the top panels of Fig. 1. We can clearly see the sharp diamagnetic drop just below 2 K for  $\text{La}_2\text{Ir}_3\text{Si}_5$  and a slightly broader one below 2.9 K for  $\text{Y}_2\text{Ir}_3\text{Si}_5$  which marks the onset of these compounds into the superconducting state respectively. The  $T_C$  for  $\text{Y}_2\text{Ir}_3\text{Si}_5$  is found to be the same as

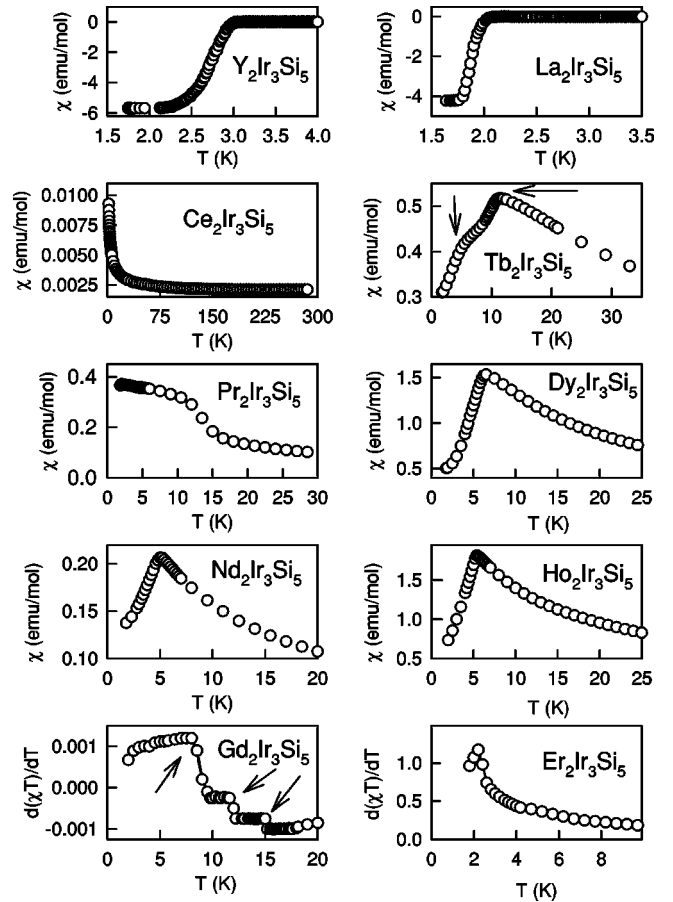


FIG. 1. The low-temperature (except for Ce) variation of susceptibility  $\chi[d(\chi T)/dT]$  for Gd and Er for the  $R_2\text{Ir}_3\text{Si}_5$  compounds. The diamagnetic drop for the Y and La samples signals the superconducting transition for these compounds, while anomalies in the susceptibility for the magnetic compounds signal the onset of magnetic ordering. The Gd and Tb compounds show multiple anomalies marked by arrows (see text for details).

has been reported in an earlier work.<sup>13</sup> The normal state  $\chi(T)$  (not shown here) of both  $\text{La}_2\text{Ir}_3\text{Si}_5$  and  $\text{Y}_2\text{Ir}_3\text{Si}_5$  is weakly paramagnetic and practically temperature independent down to low temperatures. Small upturns were seen at the lowest temperatures, which could possibly be due to trace amounts of paramagnetic impurities.

##### 2. Properties of magnetic rare-earth-containing compounds $R_2\text{Ir}_3\text{Si}_5$

The temperature dependence of the dc magnetic susceptibility for  $\text{Ce}_2\text{Ir}_3\text{Si}_5$  is also shown in Fig. 1. It can clearly be seen that  $\text{Ce}_2\text{Ir}_3\text{Si}_5$  has susceptibility values similar to those of the nonmagnetic members of this series. The susceptibility behavior is also practically temperature independent except for a small upturn at the lowest temperatures, probably due to trace amounts of paramagnetic impurities. The inverse susceptibility also does not follow a Curie-Weiss behavior in any temperature range. This would indicate that Ce is in its nonmagnetic tetravalent state in this compound. This is in contradiction to the behavior of the lattice parameters for the Ce compound, which suggests that Ce is trivalent in this

TABLE II. Parameters obtained from the high-temperature susceptibility fit to the Curie-Weiss expression given by Eq. (1).  $\mu_{th}$  is the theoretical free ion value for trivalent rare-earth ions.

Sample	$\chi_0$ (emu/mol K)	$\mu_{eff}$ ( $\mu_B$ )	$\mu_{th}$ ( $\mu_B$ )	$\theta_p$ (K)	$\mu_{Ir}$ ( $\mu_B$ )
Y <sub>2</sub> Ir <sub>3</sub> Si <sub>5</sub>	$3.371 \times 10^{-3}$				
La <sub>2</sub> Ir <sub>3</sub> Si <sub>5</sub>	$2.034 \times 10^{-3}$				
Ce <sub>2</sub> Ir <sub>3</sub> Si <sub>5</sub>	$2.115 \times 10^{-3}$				
Pr <sub>2</sub> Ir <sub>3</sub> Si <sub>5</sub>	$-1.507 \times 10^{-4}$	4.38	3.58	-21.40	2.05
Nd <sub>2</sub> Ir <sub>3</sub> Si <sub>5</sub>	$1.557 \times 10^{-4}$	3.79	3.62	-4.65	1.19
Gd <sub>2</sub> Ir <sub>3</sub> Si <sub>5</sub>	$-4.762 \times 10^{-4}$	8.14	7.94	-22.10	1.47
Tb <sub>2</sub> Ir <sub>3</sub> Si <sub>5</sub>	$-9.36 \times 10^{-4}$	9.99	9.7	-31.5	1.88
Dy <sub>2</sub> Ir <sub>3</sub> Si <sub>5</sub>	$2.913 \times 10^{-3}$	10.32	10.65	-11.81	
Er <sub>2</sub> Ir <sub>3</sub> Si <sub>5</sub>	$-3.390 \times 10^{-4}$	9.92	9.59	0.63	2.06
Tm <sub>2</sub> Ir <sub>3</sub> Si <sub>5</sub>	$-2.134 \times 10^{-3}$	7.78	7.56	2.64	1.5

compound. The high-temperature susceptibility (100 K <  $T$  < 300 K) of the other compounds containing a magnetic rare-earth element (not shown here) could be fitted to a modified Curie-Weiss expression given by  $\chi = \chi_0 + C/(T - \theta_p)$ . Here,  $\chi_0$  is the temperature-independent susceptibility (sum of the Pauli, Landau, and core susceptibilities),  $C$  is the Curie constant, and  $\theta_p$  is the Curie-Weiss temperature. The effective moment  $\mu_{eff}(\mu_B)$  can be estimated from the value of the Curie constant  $C$  as  $C \approx \mu_{eff}^2 x / 8$ , where  $x$  is the number of magnetic  $R$  ions per formula unit ( $x = 2$  for  $R_2\text{Ir}_3\text{Si}_5$ ). The values of  $\chi_0$ ,  $\mu_{eff}$ , and  $\theta_p$  estimated from this fit are given in Table II. From Table II it is clear that the estimated effective moment in most cases (except for Dy<sub>2</sub>Ir<sub>3</sub>Si<sub>5</sub>) is found to be in excess of the free ion moment of the  $R^{3+}$  ion. From Table II one can also see that the values of  $\chi_0$  for all the compounds are quite small, and hence the possibility of large paramagnetic impurities being present in the samples is remote. This might indicate that the excess paramagnetic moment that we find could be due to a contribution from Ir, i.e., Ir may have a moment in these compounds. We can estimate the Ir moment approximately as  $\mu_{Ir} = [(2\mu_{eff}^2 - 2\mu_R^2)/3]^{1/2}$ , where  $\mu_{eff}$  is the effective moment estimated from the Curie-Weiss fit of the susceptibility data and  $\mu_R$  is the theoretical moment of free  $R^{3+}$  ions. The effective Ir moment thus estimated is listed in the last column of Table II for each compound. It can be seen that the estimated contribution from Ir, although small, is not negligible and varies from sample to sample. This means that the moment on the Ir atom depends on its magnetic environment. Thus we believe that the moment on Ir is not a local moment but probably an induced one due to polarization caused by the large magnetic moment of the surrounding rare-earth ions.

Another feature of interest obtained from the susceptibility fit is the small and positive value of the  $\theta_p$ 's for the Er<sub>2</sub>Ir<sub>3</sub>Si<sub>5</sub> and Tm<sub>2</sub>Ir<sub>3</sub>Si<sub>5</sub> samples, which is in contrast to the large and negative  $\theta_p$  values for the other samples. A negative  $\theta_p$  implies the presence of antiferromagnetic correlations. We do not understand the positive value of the  $\theta_p$ 's for the Er and Tm samples at present.

The low-temperatures  $\chi(T)$  [or  $d(\chi T)/dT$ ] plots for the other magnetic compounds are also shown in Fig. 1. The

anomalies seen for most of the compounds at low temperatures are a signature of the onset of antiferromagnetic ordering in these materials. The broad feature around 12 K for the Pr<sub>2</sub>Ir<sub>3</sub>Si<sub>5</sub> sample may not actually be a magnetic transition. As we will see when we discuss our heat capacity results, Pr<sub>2</sub>Ir<sub>3</sub>Si<sub>5</sub> shows a prominent Schottky type anomaly around the same temperature, and the feature in the susceptibility could be due to this. Single prominent anomalies in  $\chi(T)$  at 4.75 K for Nd<sub>2</sub>Ir<sub>3</sub>Si<sub>5</sub>, 6.5 K for Dy<sub>2</sub>Ir<sub>3</sub>Si<sub>5</sub>, and 5.4 K for Ho<sub>2</sub>Ir<sub>3</sub>Si<sub>5</sub> signal the onset of antiferromagnetic ordering in these compounds respectively. The low-temperature  $\chi$  data (not shown here) for Gd<sub>2</sub>Ir<sub>3</sub>Ge<sub>5</sub> showed two slope changes close together around 8 K and 12 K, respectively. The plot of the derivative  $d(\chi T)/dT$  vs  $T$  (shown in Fig. 1) shows a third anomaly around 15 K. We will see later that the resistivity and heat capacity data for Gd<sub>2</sub>Ir<sub>3</sub>Ge<sub>5</sub> also show three corresponding anomalies, indicating possible multiple magnetic transitions in this compound. The  $\chi$  data for Tb<sub>2</sub>Ir<sub>3</sub>Si<sub>5</sub> also

TABLE III. Transition temperatures  $T_p$  ( $T_N$  or/and  $T_{sc}$ ) obtained from different measurement techniques. Most of them are  $T_N$  values except for the Y and La compounds.

Sample	From $\chi$	From $\rho$	From $C_p$
	$T_p$ (K)	$T_p$ (K)	$T_p$ (K)
Y <sub>2</sub> Ir <sub>3</sub> Si <sub>5</sub>	2.85 <sup>a</sup>	2.96 <sup>a</sup>	3.04 <sup>a</sup>
La <sub>2</sub> Ir <sub>3</sub> Si <sub>5</sub>	1.95 <sup>a</sup>	1.99 <sup>a</sup>	2.08 <sup>a</sup>
Ce <sub>2</sub> Ir <sub>3</sub> Si <sub>5</sub>			
Pr <sub>2</sub> Ir <sub>3</sub> Si <sub>5</sub>			
Nd <sub>2</sub> Ir <sub>3</sub> Si <sub>5</sub>	5.00	4.91	4.86
Gd <sub>2</sub> Ir <sub>3</sub> Si <sub>5</sub>	4.82, 11.16, 14.98	4.82, 11.38, 14.98	4.99, 11.76, 15.71
Tb <sub>2</sub> Ir <sub>3</sub> Si <sub>5</sub>	3.21, 10.0	3.11, 9.98	3.09, 10.12
Dy <sub>2</sub> Ir <sub>3</sub> Si <sub>5</sub>	6.35	6.27	6.13
Ho <sub>2</sub> Ir <sub>3</sub> Si <sub>5</sub>	5.38	5.21	5.14
Er <sub>2</sub> Ir <sub>3</sub> Si <sub>5</sub>	2.2	2.16	2.17
Tm <sub>2</sub> Ir <sub>3</sub> Si <sub>5</sub>			

<sup>a</sup>Superconducting transition ( $T_C$ ).

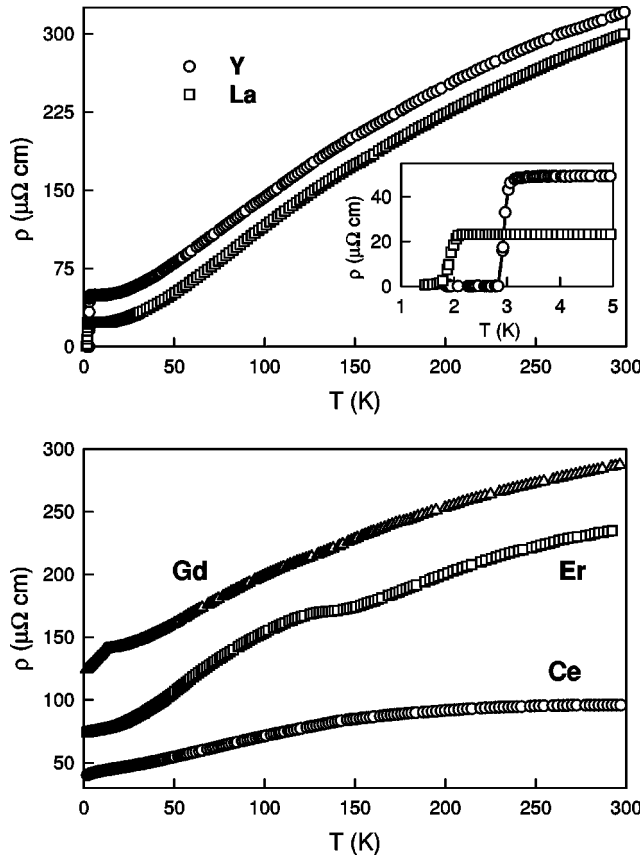


FIG. 2. Temperature dependence of resistivity ( $\rho$ ) of  $R_2\text{Ir}_3\text{Si}_5$  ( $R=\text{Y, La, Ce, Gd, and Er}$ ) from 1.5 to 300 K. The inset in the top panel shows the low-temperature  $\rho$  data for the Y and La compounds. The superconducting transitions can be clearly seen for both  $\text{Y}_2\text{Ir}_3\text{Si}_5$  ( $\approx 3$  K) and  $\text{La}_2\text{Ir}_3\text{Si}_5$  ( $\approx 2$  K).

show two distinct anomalies at 3.5 K and 10 K which are matched by anomalies in the resistivity and specific heat. The  $d(\chi T)/dT$  plot at low temperatures for  $\text{Er}_2\text{Ir}_3\text{Si}_5$  shows a clear peak just above 2 K which was not visible in the  $\chi$  vs  $T$  plot. A corresponding peak in the resistivity and heat capacity (discussed later) confirms the magnetic transition. The  $\text{Tm}_2\text{Ir}_3\text{Si}_5$  compound did not show any signature of magnetic order down to 1.8 K. The transition temperatures of the various compounds obtained from magnetic susceptibility measurements (which were determined by peaks in the  $d(\chi T)/dT$  plots) are listed in Table III, where we compare them to the temperature values of the corresponding anomalies observed in the resistivity and heat capacity measurements.

### B. Resistivity studies on $R_2\text{Ir}_3\text{Si}_5$ ( $R=\text{Y, La, Ce-Nd, Gd-Tm}$ )

The temperature dependence of the resistivity of the non-magnetic compounds  $\text{Y}_2\text{Ir}_3\text{Si}_5$  and  $\text{La}_2\text{Ir}_3\text{Si}_5$  is shown in the top panel of Fig. 2. The inset shows the low-temperature data for both compounds. The sudden drop to zero resistance indicating the transition into the superconducting state for the two compounds can be seen below 3 K and 2 K, respectively. The resistivity behavior between 1.5 K and 300 K for three magnetic compounds Ce, Gd and Er is shown in the bottom panel of Fig. 2, while the more interesting low-

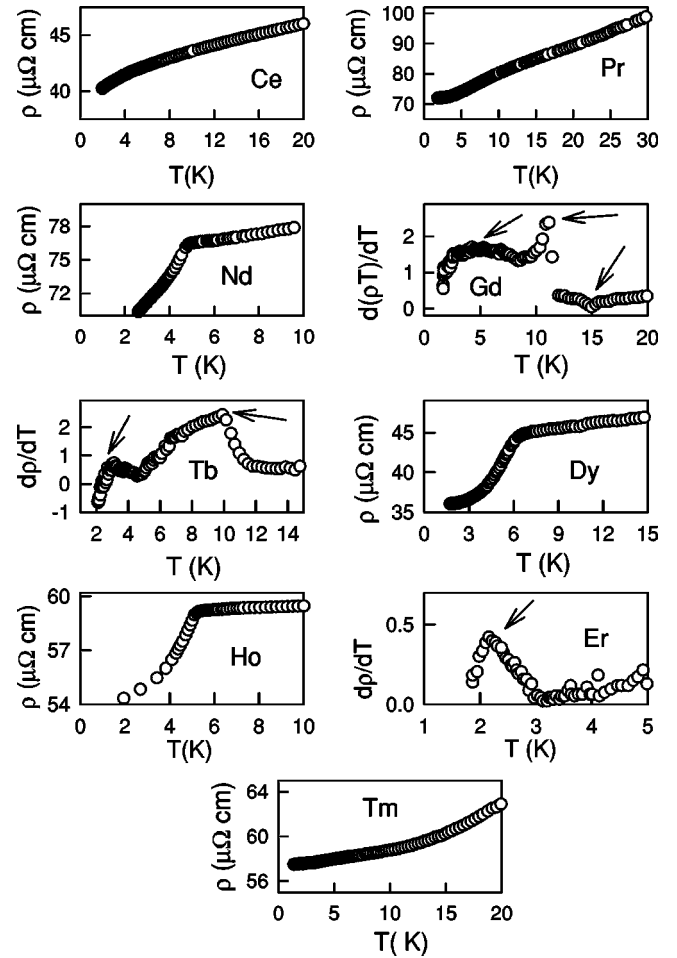


FIG. 3. The low-temperature behavior of resistivity  $\rho$  ( $dp/dT$  for Gd, Tb, and Er) of the magnetic members of  $R_2\text{Ir}_3\text{Si}_5$  to highlight the anomalies at the respective magnetic transitions.

temperature resistivity behavior for all the magnetic rare-earth-containing compounds is shown in Fig. 3.  $\text{Ce}_2\text{Ir}_3\text{Si}_5$  does not show any sign of ordering down to 1.7 K (Fig. 3) which corroborates the behavior in the susceptibility. As the temperature increases, the resistivity rapidly rises almost linearly to 150 K. For temperatures beyond 150 K (Fig. 2), it shows signs of saturating, and at the highest temperatures it does in fact saturate. This is similar to the behavior of  $\text{Ce}_2\text{Rh}_3\text{Si}_5$ ,<sup>9</sup> where the compound behaves nonmagnetically. It is possible that a Kondo minima in resistivity will be observed at higher temperatures, and what we see in the resistivity at 300 K is the coherence peak commonly seen in dense Kondo lattice systems. The large Kondo temperature  $T_K$  could be responsible for the Ce moments being compensated at 300 K itself, so that at low temperatures the compound would behave as if the Ce were nonmagnetic. This would explain the apparent contradiction between the measurement of the lattice parameters, which suggest trivalent Ce, and the susceptibility measurements, which suggest non-magnetic or tetravalent Ce in this compound. In Fig. 2 we also show the extended range of temperature dependence of the resistivity of  $\text{Gd}_2\text{Ir}_3\text{Si}_5$  as a representative plot for all the other magnetic compounds. The behavior for most of the other magnetic compounds is similar, with a slope change at



low temperatures signaling the onset of magnetic order and a high-temperature increase in the resistivity, which is slower than the expected linear rise with the resistance showing signs of saturating at higher temperatures. This behavior has been observed in other silicides and germanides among other compounds and a recent review discusses the possible mechanisms of resistivity saturation.<sup>15</sup> For the  $\text{Er}_2\text{Ir}_3\text{Si}_5$  compound (Fig. 2), we see another feature in the high-temperature resistivity data. Below 150 K a slight upturn which takes place over a temperature window of almost 20 K is observed after which the resistivity continues to drop like a metal. No obvious signature of this feature was observed in the susceptibility data for this compound. Further measurements to explore the possibility of a charge density wave or a structural transition are needed and will be carried out in the near future. None of the other compounds showed any signatures of a similar feature although the resistivity for  $\text{Dy}_2\text{Ir}_3\text{Si}_5$  (not shown here) shows an S-like shape as the temperature is increased. Let us now turn to the more interesting low-temperature resistivity behavior which we have shown in Fig. 3 for all the magnetic compounds. It can be seen that  $\text{Pr}_2\text{Ir}_3\text{Si}_5$  shows a weak shoulderlike feature around 10 K where we had observed an anomaly in the susceptibility measurement.  $\text{Tm}_2\text{Ir}_3\text{Si}_5$  does not show any signature of ordering down to the lowest temperatures of measurements. The other compounds order magnetically and the individual panels show the corresponding anomalies and slope changes at the respective magnetic transitions. For  $\text{Gd}_2\text{Ir}_3\text{Si}_5$ ,  $\text{Tb}_2\text{Ir}_3\text{Si}_5$ , and  $\text{Er}_2\text{Ir}_3\text{Si}_5$  we have shown the  $d\rho/dT$  behavior to bring out more clearly the multiple anomalies, which are otherwise not readily distinct in the  $\rho(T)$  data but are seen in the magnetic and heat capacity measurements. The transition temperatures obtained from the resistivity measurements are listed in Table III along with the values obtained from other measurements.

### C. Heat capacity studies on $R_2\text{Ir}_3\text{Si}_5$ ( $R = \text{Y, La, Ce, Nd, Gd-Tm}$ )

The temperature dependence of the heat capacity of the nonmagnetic compounds  $\text{Y}_2\text{Ir}_3\text{Si}_5$  and  $\text{La}_2\text{Ir}_3\text{Si}_5$  for low temperatures is shown in Fig. 4, plotted as  $C_p/T$  vs  $T^2$ . A sharp jump in the heat capacity at 2.8 K for  $\text{Y}_2\text{Ir}_3\text{Si}_5$  and a comparatively broader peak at 1.96 K for  $\text{La}_2\text{Ir}_3\text{Si}_5$  indicate the transition into the superconducting state for both compounds. The solid lines are fits to the expression  $C/T = \gamma + \beta T^2$ . In the normal state, the estimated values for  $\gamma_n$  (normal state value) are found to be 35 mJ/Y mol  $\text{K}^2$  and 19.4 mJ/Y mol  $\text{K}^2$  for  $\text{Y}_2\text{Ir}_3\text{Si}_5$  and  $\text{La}_2\text{Ir}_3\text{Si}_5$ , respectively. These values are quite large for nonmagnetic compounds and may possibly indicate a large density of states at the Fermi level for these compounds. The normalized jump in the heat capacity at  $T_C$ ,  $\Delta C/\gamma_n T_C$  is found to be equal to 0.85 for  $\text{Y}_2\text{Ir}_3\text{Si}_5$  and 0.41 for  $\text{La}_2\text{Ir}_3\text{Si}_5$ . These values are much reduced from the BCS value of 1.43, indicating that these compounds might be weakly coupled to intermediate-coupled superconductors. Another feature of interest in the heat capacity for these two compounds is their behavior below  $T_C$ . We found that we could fit the data below  $T_C$  also to the expression  $C/T = \gamma_{sc}$

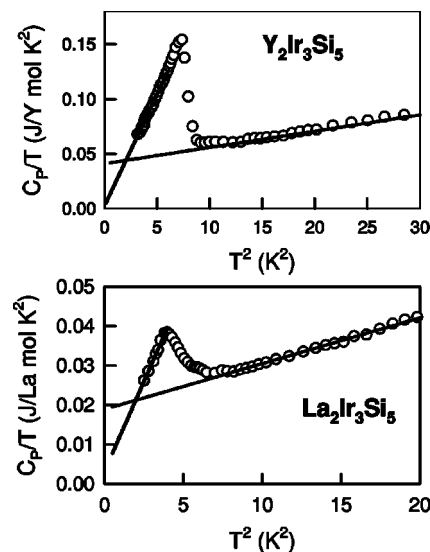


FIG. 4. The low-temperature  $C_p/T$  vs  $T^2$  data of  $\text{Y}_2\text{Ir}_3\text{Si}_5$  and  $\text{La}_2\text{Ir}_3\text{Si}_5$  compounds. The peaks indicate bulk superconductivity for both compounds. Solid lines are fits to the expression  $C_p = \gamma T + \beta T^3$  (see text for details).

+  $\beta T^2$  for both compounds. The values of  $\gamma_{sc}$  were estimated to be 8.4 mJ/Y mol  $\text{K}^2$  for  $\text{Y}_2\text{Ir}_3\text{Si}_5$ , which is about 24%  $\gamma_n$ , and 4.9 mJ/Y mol  $\text{K}^2$  for  $\text{La}_2\text{Ir}_3\text{Si}_5$ , which is again 25%  $\gamma_n$ . The reduced normalized jumps at  $T_C$  and a large linear term to the heat capacity below  $T_C$  are unusual and interesting. It could be possible that there are some amounts of impurities which stay normal and which have large  $\gamma$  values and contribute to the large linear term below  $T_C$ . However, a small value of  $\chi_0$  for all the compounds (see Table I) suggests the absence of any substantial amount of paramagnetic impurities in the samples.

A similar behavior in the superconducting state has been found for the nonmagnetic members of the series  $R_2\text{Fe}_3\text{Si}_5$ ,<sup>16</sup> where the authors explain the reduced jump in the heat capacity at the superconducting transition and a large linear term in the heat capacity below  $T_C$  by proposing a two-band model for superconductivity where one band stays normal. However, to propose that a similar scenario may be applicable for the present series, measurements down to lower temperatures are required. At present the temperature range available below  $T_C$  is quite small to make anything stronger than a suggestion.

The temperature dependence of the heat capacity for the magnetic compounds of the series are shown in Figs. 5 and 6. For clarity only the magnetic contribution ( $C_{mag}$ )/ $R$  to the heat capacity and the estimated entropy ( $S_{mag}$ )/ $R$  have been plotted ( $R$  is the universal gas constant). Also plotted for each compound is the value of the full entropy attainable [equal to  $\ln(2J+1)$ ] by the rare-earth moments with total angular momentum  $J$ . From the top panel in Fig. 5 we can clearly see that Ce does not show any signature of ordering down to 1.7 K and the heat capacity value is quite small. The inset shows the  $C_p/T$  vs  $T^2$  plot at low temperatures where the solid line is a fit to the expression  $C/T = \gamma + \beta T^2$ . At higher temperatures (not shown here) there was a slight deviation from a  $T^2$  behavior. The value for the Sommerfeld's

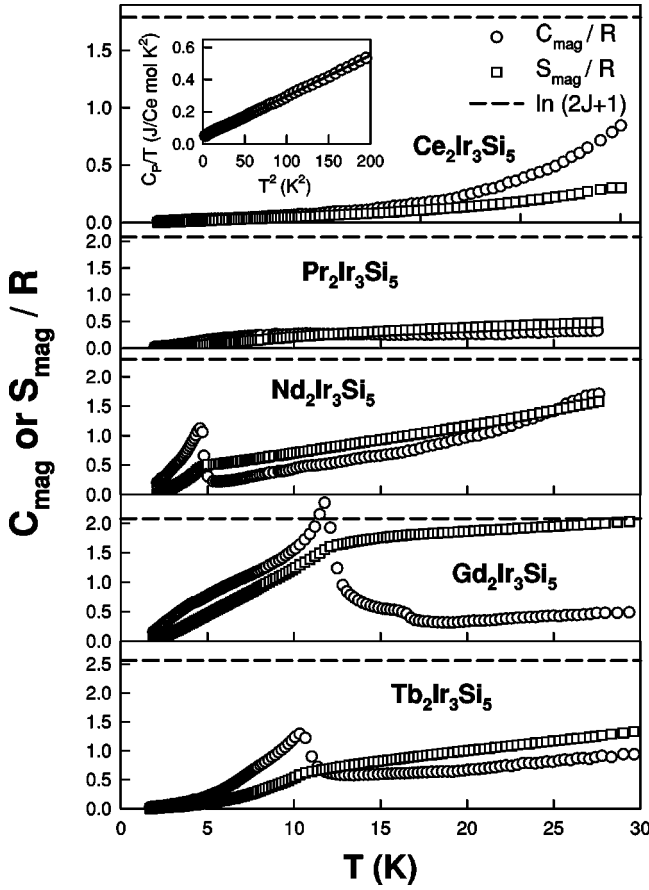


FIG. 5. Temperature dependence of the magnetic heat capacity ( $C_{mag}$ ) of  $R_2\text{Ir}_3\text{Si}_5$  ( $R=\text{Ce}, \text{Pr}, \text{Nd}, \text{Gd}, \text{and Tb}$ ) from 1.7 K to 30 K. The temperature dependence of the estimated magnetic entropy  $S_{mag}$  is also plotted in the same figure. The full theoretically expected entropy value  $\ln(2J+1)$  is also shown to compare with the final entropy actually attained (see text for details).

coefficient  $\gamma$  thus estimated comes out to be about 45 mJ/Ce mol K<sup>2</sup>. This value is of the order of the values estimated for the nonmagnetic compounds  $\text{Y}_2\text{Ir}_3\text{Si}_5$  and  $\text{La}_2\text{Ir}_3\text{Si}_5$ . This again suggests that Ce behaves as if it were nonmagnetic in this compound. We have seen from our resistivity measurements for this compound that there are indications that this could be a strongly hybridized compound with a large (close to or maybe larger than 300 K)  $T_K$  which renders the Ce moments nonmagnetic at lower temperatures. The heat capacity data for  $\text{Pr}_2\text{Ir}_3\text{Si}_5$  also do not show any signs of magnetic ordering down to the lowest temperature of measurement and may probably order below 1.7 K which was the limit of our experiment. A broad hump around 12 K in the Pr data indicates a Schottky anomaly due to the population of low-lying excited crystal field levels with increase in temperature. Due to the low-temperature tail of this anomaly, it was not possible to fit the data to estimate the Sommerfeld coefficient  $\gamma$  for this compound which would have been of interest given that now some praseodymium-based compounds also are known to show heavy electron behavior.

The temperature dependence of  $C_{mag}$  from 1.7 to 30 K of  $\text{Nd}_2\text{Ir}_3\text{Si}_5$  (Fig. 5) shows a large and distinct peak at 4.66 K,

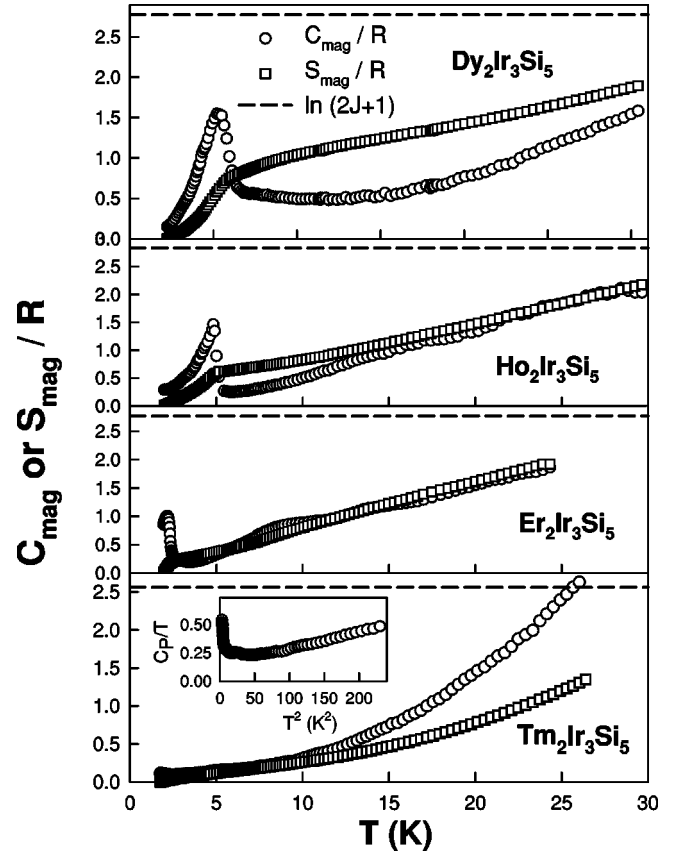


FIG. 6. Temperature dependence of the magnetic heat capacity ( $C_{mag}$ ) of  $R_2\text{Ir}_3\text{Si}_5$  ( $R=\text{Dy}, \text{Ho}, \text{Er}, \text{and Tm}$ ) from 1.7 K to 30 K. The temperature dependence of the estimated magnetic entropy  $S_{mag}$  is also plotted in the same figure. The full theoretically expected entropy value  $\ln(2J+1)$  is also shown to compare with the final entropy actually attained (see text for details). The low-temperature inset in the bottom panel for  $\text{Tm}_2\text{Ir}_3\text{Si}_5$  shows the  $C_p/T$  vs  $T^2$  data to show the onset of magnetic ordering in this compound.

which is close to the value 4.7 K found from the  $\chi(T)$  measurement. The entropy at  $T_N$  is about 80%  $R \ln 2$  which strongly suggests a doublet ground state for  $\text{Nd}_2\text{Ir}_3\text{Si}_5$ . The entropy at 30 K is much less than the expected value of  $\ln(2J+1)$  (the dashed line in the figure) which implies the presence of crystalline electric field (CEF) contributions.

For  $\text{Gd}_2\text{Ir}_3\text{Si}_5$  we observe a large  $\lambda$  type anomaly at 12 K which clearly indicates bulk magnetic ordering of  $\text{Gd}^{3+}$  moments. A broad shoulder is also visible below  $T_N$ . This could be due to reorientation of spins in the ordered state. However, a clear anomaly (at 15 K) above the main  $\lambda$  type peak suggests the existence of a different type of magnetic phase from the one into which the system orders below  $T_N$ . Three corresponding anomalies were also seen in the susceptibility and resistivity measurements, suggesting the possibility of multiple transitions in this compound. This is unusual for a Gd-based system where CEF effects are not present. The entropy for  $\text{Gd}_2\text{Ir}_3\text{Si}_5$  reaches almost its full value at  $T_N$ . The data for  $\text{Tb}_2\text{Ir}_3\text{Si}_5$  also show a shoulder at about 7 K below the main magnetic ordering peak just above 10 K. We had earlier seen signatures of these two anomalies in the susceptibility and resistivity data also. This again suggests the pos-

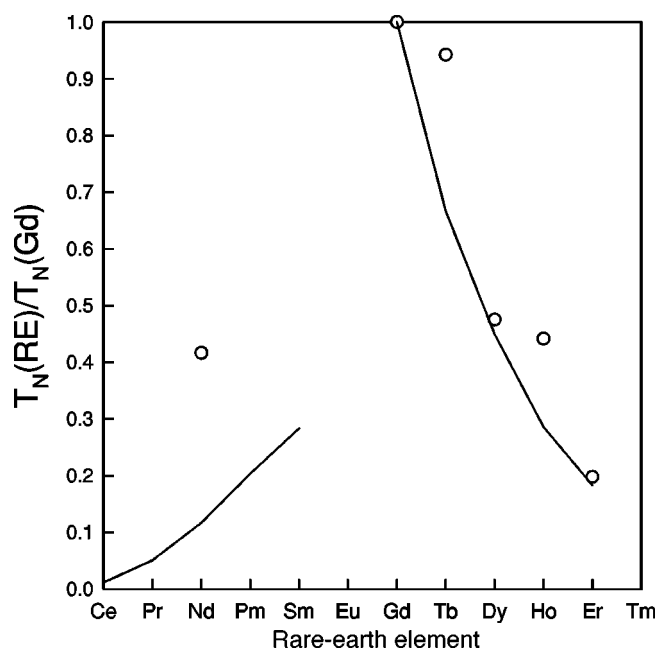


FIG. 7. Plot of the main antiferromagnetic ordering temperatures of the compounds of the series  $R_2\text{Ir}_3\text{Si}_5$  ( $R = \text{Nd}, \text{Tb}, \text{Gd}, \text{Dy}, \text{Ho}, \text{and Er}$ ) normalized to the  $T_N$  for the Gd compound. The solid lines are for the scaling law using total quantum number  $J$  (de Gennes scaling; see text for details).

sibility of multiple magnetic transitions in this compound. The entropy at  $T_N$  reaches a value of almost  $R \ln 2$  which indicates a doublet ground state for  $\text{Tb}_2\text{Ir}_3\text{Si}_5$ . Figure 6 shows the heat capacity data for the compounds  $R_2\text{Ir}_3\text{Si}_5$  ( $R = \text{Dy}, \text{Ho}, \text{Er}, \text{and Tm}$ ). The heat capacity of  $\text{Dy}_2\text{Ir}_3\text{Si}_5$  shows a distinct peak at its magnetic ordering transition. A large peak at 4.8 K indicates the onset of bulk magnetic ordering in  $\text{Ho}_2\text{Ir}_3\text{Si}_5$  (Fig. 6). From the entropies at  $T_N$  it can be deduced that both  $\text{Dy}_2\text{Ir}_3\text{Si}_5$  and  $\text{Ho}_2\text{Ir}_3\text{Si}_5$  have doublet ground states and their entropies at 30 K are much reduced from the full  $\ln(2J+1)$  value indicating crystal field effects. The heat capacity for  $\text{Er}_2\text{Ir}_3\text{Ge}_5$  shows an upturn at low temperatures starting at 3.5 K and undergoes a maximum peaked around 1.9 K. Corresponding peaks seen earlier in the  $d(\chi T)/dT$  (Fig. 1) and  $d\rho/dT$  (Fig. 3) data confirm the magnetic ordering in this compound. The entropy at  $T_N$  is smaller than  $R \ln 2$  but it must be noted that the magnetic transition is not complete and there would be a substantial contribution to the entropy from the low-temperature tail of the magnetic ordering peak when it occurs. Thus it can safely be said that the ground state for this compound also is a doublet.  $\text{Tm}_2\text{Ir}_3\text{Ge}_5$  does not order down to 1.7 K but an upturn in the low-temperature  $C_p/T$  vs  $T^2$  data (inset) signals the possible onset of magnetic ordering of  $\text{Tm}^{3+}$  moments.

In general, in the absence of CEF effects, the magnetic ordering temperatures  $T_N$  for a series of isostructural and isoelectronic metals are expected to scale (de Gennes scaling<sup>17</sup>) as  $(g_J - 1)^2 J(J+1)$  where  $g_J$  is the Landé  $g$  factor and  $J$  is the total angular momentum of the local moment. In Fig. 7 we compare the  $T_N$ 's (open circles) for the compounds that undergo magnetic ordering with the de Gennes scaling factor  $(g_J - 1)^2 J(J+1)$  normalized to the value for Gd (solid

line). It is evident that the ordering temperatures of the  $\text{Nd}_2\text{Ir}_3\text{Si}_5$  and  $\text{Tb}_2\text{Ir}_3\text{Si}_5$  compounds are anomalously large compared to the de Gennes scaling  $(g_J - 1)^2 J(J+1)$  while the  $T_N$ 's for the rest of the compounds more or less follow the scaling curve. We have seen from the heat capacity behavior of these compounds that CEF effects are important. It is known that CEF effects can lead to deviations from the de Gennes scaling and we feel that this could be the reason why the ordering temperatures of some of the compounds of the series  $R_2\text{Ir}_3\text{Si}_5$  do not follow the de Gennes scaling behavior.

#### IV. CONCLUSION

To conclude, we have synthesized and studied compounds of the series  $R_2\text{Ir}_3\text{Si}_5$  with  $R = \text{Y}, \text{La}, \text{Ce-Nd}, \text{and Gd-Tm}$  using powder x-ray diffraction, magnetic susceptibility, electrical resistivity, and heat capacity measurements down to 1.7 K. The nonmagnetic compounds  $\text{Y}_2\text{Ir}_3\text{Si}_5$  and  $\text{La}_2\text{Ir}_3\text{Si}_5$  undergo transitions into the superconducting state below 2.9 K and 2 K, respectively. Large normal state  $\gamma$  values of 35 mJ/Y mol K<sup>2</sup> and 19.4 mJ/Y mol K<sup>2</sup> for  $\text{Y}_2\text{Ir}_3\text{Si}_5$  and  $\text{La}_2\text{Ir}_3\text{Si}_5$ , respectively, suggest a large density of states at the Fermi level. A reduced jump  $\Delta C/\gamma T_C$  and a large linear term in the heat capacity below  $T_C$  is observed for these compounds and may possibly mean that some fraction of the Fermi surface does not participate in the superconductivity. However, this is just a conjecture at the present, and further studies down to lower temperatures are required before a complete understanding about this observation can be reached. For the magnetic compounds (except Ce which did not follow a Curie-Weiss behavior for any temperature range), effective moments estimated from Curie-Weiss fits to the high-temperature inverse susceptibility data are larger than the expected value for free trivalent ions. We have proposed that a moment is induced on Ir by polarization caused by the large moments of the neighboring magnetic ions. Our susceptibility and heat capacity results indicate that, in  $\text{Ce}_2\text{Ir}_3\text{Si}_5$ , Ce is in its nonmagnetic tetravalent state. However, the systematics of the lattice parameters suggest that Ce is trivalent in this compound. The resistivity for this compound shows signs of a possible Kondo effect above 300 K, suggesting that the Ce moments are strongly compensated at 300 K itself so that the compound behaves nonmagnetically at low temperatures. This behavior is similar to the compound  $\text{Ce}_2\text{Rh}_3\text{Si}_5$ ,<sup>9</sup> where the Ce moments are said to be strongly hybridized. The  $\text{Pr}_2\text{Ir}_3\text{Si}_5$  compound also does not order down to 1.7 K while the other compounds containing magnetic rare earths order antiferromagnetically at low temperatures.  $\text{Gd}_2\text{Ir}_3\text{Si}_5$  and  $\text{Tb}_2\text{Ir}_3\text{Si}_5$  compounds show more than one anomaly in the susceptibility, resistivity, and heat capacity data suggesting multiple magnetic transitions. From the temperature dependence of the entropy for the various compounds we have been able to establish that the ground state for the compounds  $\text{Nd}_2\text{Ir}_3\text{Si}_5$ ,  $\text{Tb}_2\text{Ir}_3\text{Si}_5$ ,  $\text{Dy}_2\text{Ir}_3\text{Si}_5$ ,  $\text{Ho}_2\text{Ir}_3\text{Si}_5$ , and  $\text{Er}_2\text{Ir}_3\text{Ge}_5$  is a doublet. We could also observe the complete octuplet for  $\text{Gd}_2\text{Ir}_3\text{Ge}_5$ . It was difficult to establish the ground states for the  $\text{Pr}_2\text{Ir}_3\text{Si}_5$  and the  $\text{Tm}_2\text{Ir}_3\text{Si}_5$  compounds given that the Pr compounds do not order down to the lowest temperatures of our measurements and for the

Tm compound the magnetic transition was not complete down to the lowest temperature of measurement. An upturn seen in the resistivity of  $\text{Er}_2\text{Ir}_3\text{Si}_5$  below 150 K possibly suggests a partial gapping of the Fermi surface. However, the nature of this anomaly could not be identified at present. Finally, the transition temperatures for most of the com-

pounds scale with the de Gennes factor, indicating that the primary mechanism which leads to the ordering of the magnetic moments may be the usual Ruderman-Kittel-Kasuda-Yosida type of indirect exchange, and any deviation from this scaling is probably due to strong CEF effects, as are evident from our heat capacity results.

- 
- <sup>1</sup>P. Rogl, in *Handbook of Physics and Chemistry of Rare Earths*, edited by K. A. Gschneidner, Jr. and L. Eyring (Elsevier Science Publishers/North-Holland, Amsterdam, 1984), Vol. 7, pp. 1–264.
- <sup>2</sup>J. Leciejewicz and A. Szytula, in *Handbook of Physics and Chemistry of Rare Earths*, edited by K. A. Gschneidner, Jr. and L. Eyring (Elsevier Science Publishers/North-Holland, Amsterdam, 1989), Vol. 12, p. 133.
- <sup>3</sup>C. B. Vining and R. N. Shelton, Phys. Rev. B **28**, 2732 (1983).
- <sup>4</sup>H. F. Braun, Phys. Lett. **75A**, 386 (1980).
- <sup>5</sup>H. F. Braun, C. U. Segre, F. Acker, M. Rosenberg, S. Dey, and U. Deppe, J. Magn. Magn. Mater. **25**, 117 (1981).
- <sup>6</sup>A. R. Moodenbaugh, D. E. Cox, and H. F. Braun, Phys. Rev. B **25**, 4702 (1981).
- <sup>7</sup>S. Noguchi and K. Okuda, Physica B **194-196**, 1975 (1994).
- <sup>8</sup>C. Mazumdar, K. Ghosh, R. Nagarajan, S. Ramakrishnan, B. D. Padalia, and L. C. Gupta, Phys. Rev. B **59**, 4215 (1999).
- <sup>9</sup>S. Ramakrishnan, N. G. Patil, A. D. Chinchure, and V. R. Marathe, Phys. Rev. B **64**, 064514 (2001).
- <sup>10</sup>N. G. Patil and S. Ramakrishnan, Phys. Rev. B **59**, 12 054 (1999).
- <sup>11</sup>Yogesh Singh and S. Ramakrishnan, Phys. Rev. B **68**, 054419 (2003).
- <sup>12</sup>Yogesh Singh and S. Ramakrishnan, Phys. Rev. B **69**, 174423 (2004).
- <sup>13</sup>M. Hirjak, P. Lejay, B. Chevalier, J. Etourneau, and P. Hagemmuller, J. Less-Common Met. **105**, 139 (1985).
- <sup>14</sup>C. Godart, C. V. Tomy, L. C. Gupta, and R. Vijayraghavan, Solid State Commun. **67**, 677 (1988).
- <sup>15</sup>O. Gunnarsson, M. Calandra, and J. E. Han, Rev. Mod. Phys. **75**, 1085 (2003).
- <sup>16</sup>C. B. Vining, R. N. Shelton, H. F. Braun, and M. Pelizzone, Phys. Rev. B **27**, 2800 (1983).
- <sup>17</sup>D. R. Noakes and G. K. Shenoy, Phys. Lett. **91A**, 35 (1982).